Upscaling production of droplets and magnetic particles with additive manufacturing

Donatien Mottin
University of Alberta, Edmonton, Canada and University of Rennes 1, Rennes, France, and
Tsaihsing Martin Ho and Peichun Amy Tsai
University of Alberta, Edmonton, Canada

Abstract

Purpose – Monodisperse microfluidic emulsions – droplets in another immiscible liquid – are beneficial to various technological applications in analytical chemistry, material and chemical engineering, biology and medicine. Upscaling the mass production of micron-sized monodisperse emulsions, however, has been a challenge because of the complexity and technical difficulty of fabricating or upscaling three-dimensional (3 D) microfluidic structures on a chip. Therefore, the authors develop a fluid dynamical design that uses a standard and straightforward 3 D printer for the mass production of monodisperse droplets.

Design/methodology/approach – The authors combine additive manufacturing, fluid dynamical design and suitable surface treatment to create an easy-to-fabricate device for the upscaling production of monodisperse emulsions. Considering hydrodynamic networks and associated flow resistance, the authors adapt microfluidic flow-focusing junctions to produce (water-in-oil) emulsions in parallel in one integrated fluidic device, under suitable flow rates and channel sizes.

Findings – The device consists of 32 droplet-makers in parallel and is capable of mass-producing 14 L/day of monodisperse emulsions. This convenient method can produce 50,000 millimetric droplets per hour. Finally, the authors extend the current 3 D printed fluidics with the generated emulsions to synthesize magnetic microspheres.

Originality/value – Combining additive manufacturing and hydrodynamical concepts and designs, the authors experimentally demonstrate a facile method of upscaling the production of useful monodisperse emulsions. The design and approach will be beneficial for mass productions of smart and functional microfluidic materials useful in a myriad of applications.

Keywords Design, Mechanical engineering, Rapid manufacturing, Manufacturing, Engineering, Prototyping, 3 D Printing, Additive manufacturing, Flow-focusing, Magnetic particles, Monodisperse emulsions, Mass production

Paper type Research paper

1. Introduction

With recent advances in micro- and nano-fabrication, microfluidics has become a promising and enabling platform and toolbox for a wide range of fields, such as biology, medicine, fluid physics, analytical chemistry, chemical and material engineering, as well as micro-electro-mechanical systems (Tabeling, 2005; Weibel and Whitesides, 2006; Whitesides, 2006). Some useful applications and examples include smart capsule synthesis for targeted drug delivery (Seiffert *et al.*, 2010), microfluidic channels for detecting the serological status of a subject (Cheng *et al.*, 2007), microfluidic networks mimicking human organs to test new treatments (Bhise *et al.*, 2014) and microfluidic devices for making novel material and objects. Moreover, with the handy and precise controls of fluids and chemical reactions, microfluidics has recently enabled the easy fabrications of a variety of functional microscale objects.

Miniature droplets created by microfluidics are particularly of interest and can be beneficially used as templates to design complex materials (Romanowsky *et al.*, 2012). For example, simple emulsions are used as a precursor to metal nanoparticles (Wagner *et al.*, 2008) or polymerized Janus microparticles (Chen *et al.*, 2009). More complex objects can be obtained using double emulsions (Datta *et al.*, 2014; Nawar *et al.*, 2020), such as microcapsules for delivering drugs in the organism (Ren *et al.*, 2010; Zhang *et al.*, 2012) or stable gas-filled microcapsules as contrast enhancers for acoustic imaging in porous media (Abbaspourrad *et al.*, 2013; Lee *et al.*, 2010).

Microfluidic devices are now widely used in the research field for many synthesis applications but rarely in the industry because of their low production rates. High throughput is currently one of the most significant limitations of microfluidic

The current issue and full text archive of this journal is available on Emerald Insight at: **https://www.emerald.com/insight/1355-2546.htm**

Rapid Prototyping Journal
27/9 (2021) 1693–1699
© Emerald Publishing Limited [ISSN 1355-2546]
[DOI 10.1108/RPJ-12-2020-0320]

Conflicts of interest: There are no conflicts to declare.

The authors acknowledge the support from Canada First Research Excellence Fund (CFREF), Future Energy System (FES) at the University of Alberta, and Canada Foundation for Innovation (CFI). The author Peichun Amy Tsai holds a Canada Research Chair in Fluids and Interfaces and thankfully acknowledges Natural Sciences and Engineering Research Council (NSERC) of Canada via the Discovery and Accelerator grants.

Received 26 December 2020
Revised 22 April 2021
Accepted 26 May 2021

devices. Due to the tiny amount of fluid contained in a microfluidic device (e.g. a few pL), the production of one microfluidics droplet-maker is rather low. To make microfluidic devices worthwhile in an industrial production chain, improving the throughput is essential. To overcome this limitation, much recent research has focused on the assembly of multiple paralleled droplet-makers to increase the global production rate of droplets.

Recently, there have been multiple strategies proposed to resolve the limitation of low mass production of microfluidic emulsions. Some innovative examples include centrosymmetric designs (Nisisako *et al.*, 2012; Nisisako and Torii, 2008), paralleled step channel designs using a hydrodynamic instability (Amstad *et al.*, 2016) and a more efficient method using paralleled flow-focusing junctions (Jeong *et al.*, 2015; Romanowsky *et al.*, 2012). A flow-focusing junction consists of one central channel intersecting with two side channels. The central liquid is pinched by another liquid from both sides, leading to droplet formation via a hydrodynamic instability. One typical flow-focusing junction hence requires two (liquid) inlets and one (droplet) outlet with a planar design. Therefore, two-dimensional models of flow-focusing are commonplace in microfluidics because of their relatively straightforward microfabrication methods.

Parallelizing of multiple flow-focusing components would require that two separate general inlets connect all flow-focusing junctions, and all produced droplets are recovered in one general outlet. However, it is not feasible to connect the three general channels (of inlets/outlets) to multiple flow-focusing junctions without crossing the general liquid distribution lines in a planer design (Vladisavljevic *et al.*, 2013). Therefore, the third dimension is essential and required to parallelize such a system. Nevertheless, such three-dimensional (3 D) microfluidic structures are complex to fabricate using the standard microfabrication techniques as the procedures involve multiple microfabrication steps, specific mask aligners and tedious alignments for photolithography. 3 D printing technology can be a convenient way to overcome this obstacle by allowing a rapid, easy and reproducible production of devices in 3 D. One of such pioneer work on the scale-up of 3 D printed flow-focusing junction was done by Femmer *et al.* (2015), whereas other 3 D printed scale-up systems have been made (Zhang *et al.*, 2019), e.g. using coaxial capillaries (Jans *et al.*, 2019) or multiple (three-parallel-united) drop makers (Kamperman *et al.*, 2020).

Despite significant applications of both 3 D printing technologies and microfluidic droplets (Suea-Ngam *et al.*, 2019), so far, there are a small number of studies reporting feasible scale-up productions of monodisperse droplets using additive manufacturing (Femmer *et al.*, 2015; Kamperman *et al.*, 2020; Zhang *et al.*, 2019, 2016), whereas very recently there has been active research on 3 D printing modules, fittings, components of microfluidic chips or a drop generator (Ji *et al.*, 2018; Nielsen and Woolley, 2020; Vijayan and Hashimoto, 2019). In this paper, we present a systematic and straightforward method to design and to produce a paralleled milli-fluidic droplet-maker device in a reproducible way, using 3 D printing (Figure 1). Hydrodynamic principles are used for the fluidic design, enabling a stable and reproducible generation of monodisperse droplets. We illustrate our method

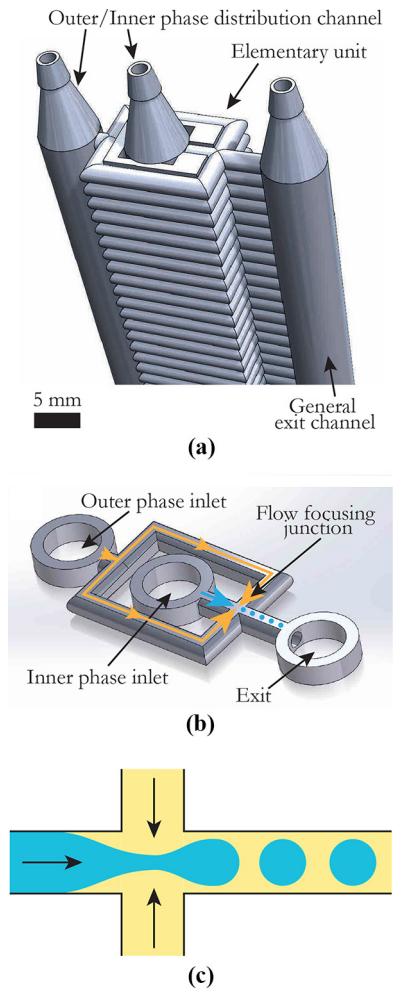

Figure 1 (a) SolidWorks illustration of our device design. Thirty-two elementary units, with two entries and one exit each, are connected via three large perpendicular distribution channels. (b) Fluidic design of one elementary unit of flow-focusing junction. The outer (oil) phase is injected via the left entry. The outer phase (→) is split in two and subsequently reconnected at the flow-focusing junction, where it meets the inner flow of the aqueous phase (→) injected from the center. Droplets are then created and collected via an exit channel on the right under certain flow conditions. (c) Sketch of the drop formation mechanism using a flow-focusing junction when the inner phase is pinched by the outer phase from both sides

using a real device composed of 32 flow-focusing junctions in parallel, which can facilitate the mass production of 50,000 droplets per hour with a diameter of 1.1 mm and dispersion of 7.1%. We further explain other design considerations when using such a device to reduce the radius dispersion of the emulsions produced. Finally, we also demonstrate the industrial application of this device by using it to make magnetic particles at an industrial production rate.

2. Materials

2.1 device fabrication

The device is first designed using SolidWorks and subsequently printed using a FormLabs 3 D Printer, based on a

photopolymerizable resin triggered by a laser spot. Once printed, the device is washed during 20 min in isopropanol, flushed by distilled water and finally dried using compressed air. Subsequently, a hydrophobic coating is applied by immersing the device during 60 s in a solution of 0.2% (v/v) of trichloro(octadecyl)silane (OTS) in toluene under magnetic agitation.

2.2 Liquids

The device is designed to produce water-based droplets (with the hydrophobic coating on the device channel). It requires an organic outer phase with a surfactant and an aqueous inner phase. Laminar flows are needed to generate reproducible droplets. To reach a higher throughput and higher liquid velocity, we used viscous fluids to ensure laminar flow regime. The inner phase is a mixture of glycerol and water (volume fraction 55% and 45%, respectively) with a dye, of final dynamic viscosity $\mu_i = 10$ cP (Cheng, 2008). The outer phase is heavy mineral oil (Sigma Aldrich) of dynamic viscosity $\mu_o =$ 130 cP, with 10% (v/v) of Span 80 as a surfactant. These fluids are injected precisely in the flow-rate range of 3×10^{-3} −64 mL/min using syringe pumps (Chemyx). Because of electrostatic repulsion, ionic surfactants (e.g. Sodium dodecyl sulfate) can be used instead to prevent droplet coalesce after the formation of droplets, stored in a container for later use.

2.3 Image capture and analysis

For imaging and polydispersity measurements, the produced emulsion is collected at the exit of the device on a microscope slide and observed using a microscope (Zeiss Axio Imager M2). Image analysis is done with ImageJ (Rasband *et al.*, 1997).

3. Design and utilization

3.1 Device description

Our droplet-making device is composed of an elementary unit repeated 32 times, shown in Figure 1. Figure 1(b) schematically shows the elementary module, consisting of a planar flow-focusing junction with two entries and one exit. A flow-focusing junction, as shown schematically in Figure 1(c), is a typical method to produce droplets in microfluidics. The inner aqueous liquid phase, which does not wet the walls, is pinched by two perpendicular flows of the outer organic phase via a Rayleigh–Plateau instability. This hydrodynamic instability makes an initial cylindrical-shaped flow into a collection of droplets because of surface tension effect. Several elementary units are stacked along the channel axial direction, and all the entries/exits of one type are connected using a large distribution channel. Illustrated in Figure 2(a) is a general sketch of the connections of the device, consisting of the inner phase of the aqueous solution, the outer phase of organic oil and the production exit for the emulsion stream.

To use the device, the inner and outer phase inlets are connected to syringe pumps. Liquids fill the main distribution channels, and subsequently fill the elementary units, and droplets are produced in parallel, collected in the common exit channel and finally leave the device.

Figure 2 (a) Schematic diagram of the fluidic network pattern of the device. (b) Hydrodynamic resistance network model considered for the device for each phase. Ru represents the hydrodynamic resistance of the elementary unit seen by the inner or outer phase; the detailed sketches of Ru are depicted for the inner phase (blue shade, R_u^i) and outer phase (orange shade, R_u^o) in (a1) and (a2), respectively. Rd represents the hydrodynamic resistance of a portion of the distribution channel (of the production exist stream or the inner/outer injection solution) between two elementary unit entries. For one elementary unit, the Rd contributions are illustrated for the inner phase (by two white dashed lines, each indicating R_d^i) and for the outer phase (by two grey dashed lines, each indicating R_d^o) in (a1) and (a2), respectively

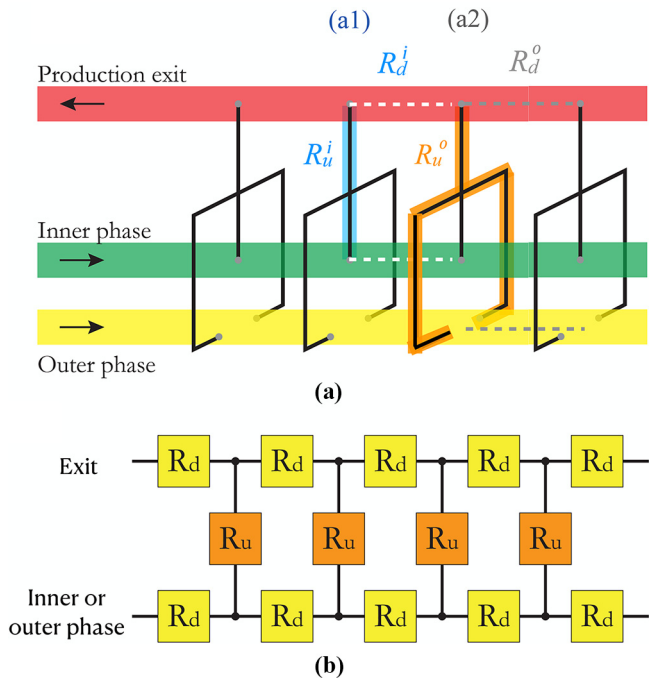

3.2 hydrodynamic considerations

The working principle of a flow-focusing junction is based on hydrodynamic instability. Therefore, a detailed understanding of the flow behavior within the device is necessary to achieve functional and efficient parallelization. To ensure a correct parallelization of the device, one needs to consider the underlying hydrodynamics, discussed below.

First, as droplets diameters are influenced by the flow rates of the inner and outer phases, we need to consider a parallelization strategy. More specifically, one has to limit flow rate differences between the elementary units to ensure the smallest polydispersity.

We resolve this by adapting the strategy proposed by Romanowsky *et al.* (2012) considering the hydraulic resistances for a pipe network. In analogy to electric resistances, a micro/milli-fluidic system can be modeled as a network of pipe-flows with hydraulic resistances (Tabeling, 2005). The electric Ohm law of electric voltage, U, is the product of electric resistance (R) and current (I), i.e. $U = RI$. In analogy, for a network of viscous internal flow, the pressure difference between the two points, ΔP, is the product of the hydraulic resistance (R_h) times the flow rate (Q) in this section of the channel, i.e. $\Delta P = R_h Q$. The hydraulic resistance of a single circular pipe of length (L)

and diameter (D) filled with a liquid of viscosity (μ) can be analytically modeled as $R_h = (128\mu L)/(\pi D^4)$ for the laminar regime of a pipe flow.

We can use the same laws of combination of resistance in series and in parallel as those for an electrical resistance network for our fluidic system of laminar viscous pipe flows. We can model the liquid distribution using a resistance model if we neglect the interaction between the two liquids, including droplet formation. For each of the two injection liquids, we model their pathway by the resistance network of Figure 2(b), in which R_d is the resistance of a section of distribution/exit channel between two units (of length L_d and diameter D_d) and R_u is the resistance of an elementary unit (of channel diameter D_u). Using the electric resistance combination laws, we can show that the flow rates of the considered liquid in the first and in the N-th elementary unit of droplet-maker are linked by:

$$Q_1 = \left(1 + 2(N-1)\frac{R_d}{R_u}\right) Q_N. \quad (1)$$

We can define $\epsilon = \frac{Q_1 - Q_N}{Q_N}$, the relative variation in the flow rates between the first and the last droplet-makers. To ensure a similar flow rate for all units, it would require $\epsilon \ll 1$ for both liquids. Therefore, for each injected liquids (i.e. inner or outer phase), denoting L_u as the length traveled by the liquid between the entry of the unit and the flow-focusing junction, we would ensure as follows:

$$\epsilon = 2(N-1)\frac{L_d}{L_u}\left(\frac{D_u}{D_d}\right)^4 << 1. \quad (2)$$

In our case, D_u = 1.5 mm, D_d = 7 mm and L_d = 3 mm. For the inner phase, $L_{u,in}$ = 4 mm; for the outer phase, $L_{u,out}$ = 25 mm. Our fluidic parameters above give rise to ϵ = 0.1 for the inner phase and ϵ = 0.015 for the outer phase, which adequately fulfills the criterion of small ϵ. The monodispersity might be further improved by reducing the inner phase ϵ. One efficient and promising way to improve this system will be to reduce D_u, which will be highly feasible in the future thanks to improvements in small-scale additive manufacturing techniques.

Once the parallelization strategy is implemented, we need to consider and deal with the effect of gravity. Contrary to standard microfluidic devices, in which gravity is commonly neglected compared to other forces (Tabeling, 2005), in our millifluidic device, the volume of liquid is large enough for the gravity to play a role. The gravitational effect has two direct consequences to our fluidic design and operation. First, if the distribution channel is not placed horizontally, hydrostatic pressure would modify the parallelization equilibrium. The pressure at some (flow-focusing) unit entries will be higher than that at some other, leading to unbalanced flow rates and hence polydispersity of the droplets. Second, our inner fluid is denser than our outer fluid. If the large distribution channels are located on top of the large exit channel, the inner fluid may flow in the flow-focusing junction because of buoyancy and not because of flow pressure. The latter situation would make the drop formation process unstable. Hence, if the inner phase is denser than the outer phase, the device must be oriented in a specific way that the distribution channels are under the general exit channel, as illustrated in Figure 4(a).

Finally, the last issue to deal with concerns the bubbles. Due to the large volume of gas in the device initially, the size of the channels and the flow complexity inside the device, bubble trapping inside the device is unavoidable. This issue can be solved by adding additional (anti-bubble) exits at the end of the large distribution channels, as depicted in Figure 4(a). When the device is first filled, these exits are open allowing the gas present in the device to flow out. Once the distribution channels are completely full of liquid, with no more bubbles in it, the anti-bubble exit valves are closed manually. The liquid subsequently flows in the elementary units, ensuring a continuous liquid flow without bubbles.

4. Results and application

4.1 Droplet production: phase diagram

To forecast the type of flow that will occur in the device, we map out the flow regimes for various flow rates (controlled by the syringe pumps) in a single elementary unit of flow-focusing, whose geometry and channel size are identical to those depicted in Figure 1(b). The primary procedures include first, filling the outer phase with a flow rate (Q_o), subsequently injecting the inner phase at a flow rate (Q_i) and observing the resultant flow pattern in the outlet channel. If the inner phase has not wetted the walls, one of the two flow rates is modified to map out the flow pattern phase diagram of Figure 3(a). Otherwise, if the inner phase wets the wall, we stop the experiment with this system and use a new device (or wash it and reapply the surface treatment) to ensure the hydrophobic coating on the channel wall. Figure 3(a) shows the experimental result of the phase diagram of diverse flow configurations observed in one elementary flow-focusing junction. During the utilization of the device, four flow regimes were observed, sketched in Figure 3(b) the dripping state (where the droplet forms at the intersection of the flow-focusing junction), the jetting state (where tiny droplet forms downstream of the junction), the co-flow state (where no droplets are formed) and the gravity blocking state (where the denser inner phase is stuck at the bottom of the device due to gravity).

As shown in Figure 3(a), for low inner phase flow rates, the flow pressure is not strong enough to overcome gravity. The denser inner phase thus flows down via the outer phase channel. This is the *gravity blocking state*. For high inner phase but low outer phase flow rates, the inner phase flow is unaffected by the quasi-static outer phase flow, thereby in the *co-flow state*. If the two flow rates are roughly balanced, the inner phase is injected in the junction. When it begins to obstruct the exit, the outer phase flow pushes the inner phase, pinching it, cutting the stream and creating a droplet. This is the desired *dripping state*. Finally, if both flow rates are high, a co-flow is metastable, but the jet destabilizes into tiny droplets after a small distance, as the *jetting state*.

4.2 Production rate and size distribution

The device is used with an inner flow rate of 0.64 mL/min and an outer flow rate of 9.6 mL/min, which corresponds to the dripping state for a device with 32 units. A video of the working fluidics is available in supplementary materials. The produced emulsion is observed via a reflective

Figure 3 (a) Phase diagram of the droplet production regime in our case. Indicated flow rates are those passing through one elementary unit, which corresponds to the total flow rate divided by the number of elementary units. (b) Sketch of the four possible states of flow configurations under different inner and outer flow rates: dripping (●), jetting (◆), co-flow (■) and gravity blocking (▼) observed in one elementary flow-focusing junction of our device

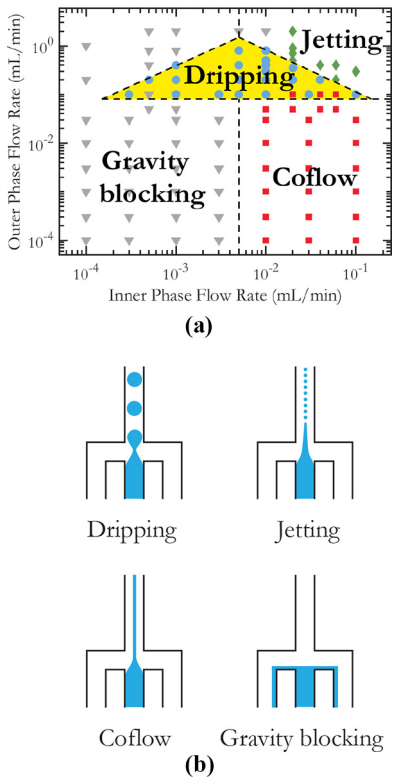

microscope [Figure 4(b)], and the images are analyzed using ImageJ. The histogram of the resultant droplet diameter is shown in Figure 4(c). We measured a mean diameter of 1.1 mm and a relative standard deviation of 7.1%, representing a good monodispersity. Using this set of parameters, we can produce 14 L/day of water-in-oil emulsions, which corresponds to 50,000 droplets per hour.

4.3 Synthesis of magnetic particles

As an application, we used this device to synthesize magnetic particles, inspired by the protocol described in the study of Zhang *et al.* (2012). To make magnetic particles, the inner phase is polyethylene glycol (PEG) diacrylate (Sigma-Aldrich) with 5% (v/v) 20 nm PEG-COOH-coated nanomagnetic particles solution (Micromod Partikeltechnologie GmbH) and 2% (w/w) 2,2-dimethoxy-2-phenylacetophenone (Sigma-Aldrich) as polymerization photoinitiator. The outer phase is 130 cP heavy mineral oil (Fisher Scientific) with 10% (v/v) of Span 80 as a surfactant. Both phases are injected into the device at a flow rate of 1.12 mL/min and 19.2 mL/min, respectively. The produced droplets are then collected in a petri dish and placed under ultraviolet light (254 nm) for 5 min to trigger the polymerization of PEG diacrylate. Droplets subsequently

Figure 4 (a) Photograph of the actual device as it is used. (b) Microscope image of water-in-oil emulsions produced by the 3 D printed device. (c) Distribution of droplet diameter of the produced emulsions

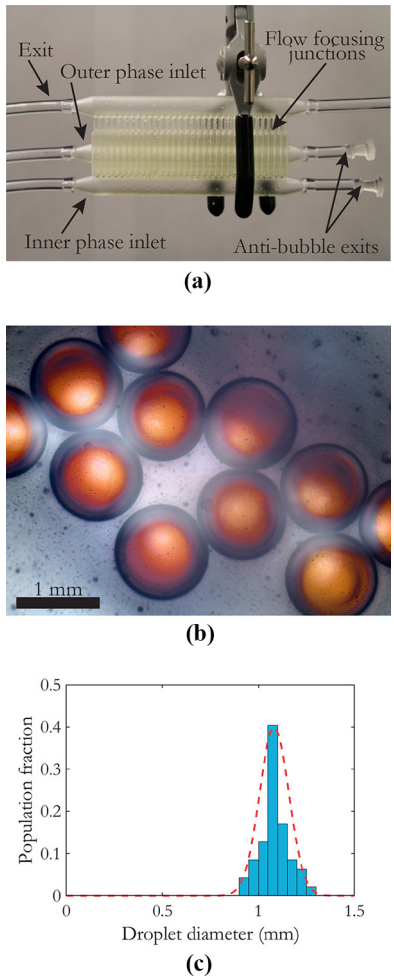

solidify and turn into solid particles with magnetic nanoparticles trapped inside.

A microscope image of the produced magnetic particles is presented in Figure 5(a). With this set of parameters, 2,000,000 droplets of 1.1 mm can be synthesized per day. To further prove the magnetic property of such particles, we put the synthesized magnetic particles into a water channel, which is next to a magnet at 11.5 mm away. The records of the trajectories are shown in Figure 5(b) and 5(c). The trajectory is downward due to gravity but is deflected by the presence of the magnet force toward the right.

5. Conclusions

We present a simple, useful and systematic 3 D printing method to fabricate a milli-fluidic device of upscaling, parallelized droplet-makers, with massive throughput and high monodispersity. With hydrodynamic considerations and concepts, we demonstrate this method's feasibility and reliability by producing a 32-droplet-maker device, which can produce 50,000 droplets of diameter 1.1 mm per hour with a dispersion of 7.1%. We show that channel dimensions are

Figure 5 (a) Microscope image of our synthesized magnetic particle. (b) Overlay of photographs of a synthesized magnetic particle in water, next to a (rare-earth) magnet. The magnetic particle falls because of gravity but is deflected due to the presence of the magnet. (c) Plot of the trajectories of several magnetic particles in similar conditions. The final drift slope is identical for all particles, proving the similarity in magnetic property value between the particles

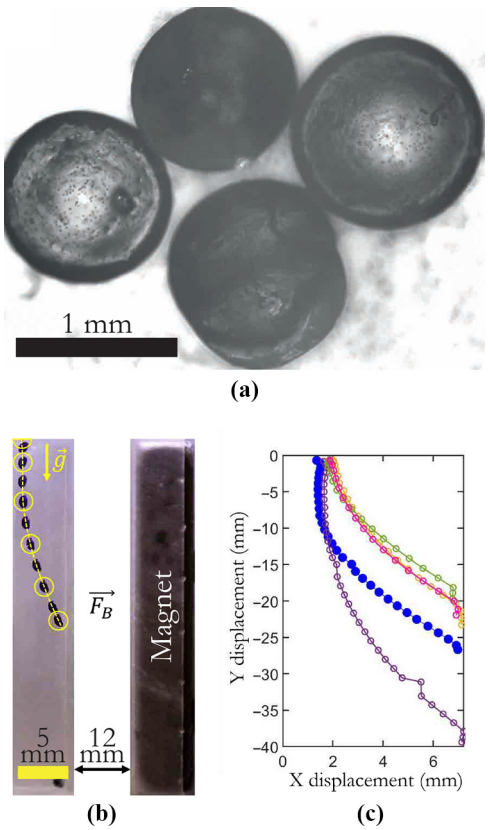

critical for creating an effective parallelization system. Moreover, bubbles, gravity and surface property must be taken into account by implementing bubble exits in the channel design, orienting the device properly during utilization and applying an inner surface coating to avoid unwanted wall wetting, respectively. We also use this upscaling device to produce magnetic milli-particle at high throughput. Finally, further improvement for this method will involve smaller printing sizes, especially smaller channel diameter. In fact, reducing channel sizes will facilitate all the processes beneficially: the ϵ parameter will be lower, and all volume forces (e.g. gravity) will progressively fade out. A smaller channel will also reduce the Reynolds number, which will allow the use of less viscous liquids and hence higher flow velocity and throughput.

References

Abbaspourrad, A., Duncanson, W.J., Lebedeva, N., Kim, S. H., Zhushma, A.P., Datta, S.S., Dayton, P.A., Sheiko, S.S., Rubinstein, M. and Weitz, D.A. (2013), "Microfluidic fabrication of stable gas-filled microcapsules for acoustic contrast enhancement", *Langmuir*, Vol. 29 No. 40, pp. 12352-12357.

Amstad, E., Chemama, M., Eggersdorfer, M., Arriaga, L.R., Brenner, M.P. and Weitz, D.A. (2016), "Robust scalable high throughput production of monodisperse drops", *Lab on a Chip*, Vol. 16 No. 21, pp. 4163-4172.

Bhise, N.S., Ribas, J., Manoharan, V., Zhang, Y.S., Polini, A., Massa, S., Dokmeci, M.R. and Khademhosseini, A. (2014), "Organ-on-a-chip platforms for studying drug delivery systems", *Journal of Controlled Release*, Vol. 190, pp. 82-93.

Chen, C.H., Shah, R.K., Abate, A.R. and Weitz, D.A. (2009), "Janus particles templated from double emulsion droplets generated using microfluidics", *Langmuir*, Vol. 25 No. 8, pp. 4320-4323.

Cheng, N.S. (2008), "Formula for the viscosity of a glycerol-water mixture", *Industrial & Engineering Chemistry Research*, Vol. 47 No. 9, pp. 3285-3288.

Cheng, X., Irimia, D., Dixon, M., Sekine, K., Demirci, U., Zamir, L., Tompkins, R.G., Rodriguez, W. and Toner, M. (2007), "A microfluidic device for practical label-free cd4+ *t* cell counting of hiv-infected subjects", *Lab Chip*, Vol. 7 No. 2, pp. 170-178.

Datta, S.S., Abbaspourrad, A., Amstad, E., Fan, J., Kim, S.H., Romanowsky, M., Shum, H.C., Sun, B., Utada, A.S., Windbergs, M., Zhou, S. and Weitz, D.A. (2014), "25th anniversary article: double emulsion templated solid microcapsules: mechanics and controlled release", *Advanced Materials*, Vol. 26 No. 14, pp. 2205-2218.

Femmer, T., Jans, A., Eswein, R., Anwar, N., Moeller, M., Wessling, M. and Kuehne, A.J. (2015), "High-throughput generation of emulsions and microgels in parallelized microfluidic drop-makers prepared by rapid prototyping", *ACS Applied Materials & Interfaces*, Vol. 7 No. 23, pp. 12635-12638.

Jans, A., Lölsberg, J., Omidinia-Anarkoli, A., Viermann, R., Möller, M., De Laporte, L., Wessling, M. and Kuehne, A.J. C. (2019), "High-throughput production of micrometer sized double emulsions and microgel capsules in parallelized 3d printed microfluidic devices", *Polymers*, Vol. 11 No. 11, p. 1887.

Jeong, H.H., Yelleswarapu, V.R., Yadavali, S., Issadore, D. and Lee, D. (2015), "Kilo-scale droplet generation in three-dimensional monolithic elastomer device (3d med)", *Lab on a Chip*, Vol. 15 No. 23, pp. 4387-4392.

Ji, Q., Zhang, J., Liu, Y., Li, X., Lv, P., Jin, D. and Duan, H. (2018), "A modular microfluidic device via multimaterial 3d printing for emulsion generation", *Scientific Reports*, Vol. 8 No. 1, p. 4791.

Kamperman, T., Teixeira, L.M., Salehi, S.S., Kerckhofs, G., Guyot, Y., Geven, M., Geris, L., Grijpma, D., Blanquer, S. and Leijten, J. (2020), "Engineering 3d parallelized microfluidic droplet generators with equal flow profiles by computational fluid dynamics and stereolithographic printing", *Lab on a Chip*, Vol. 20 No. 3, pp. 490-495.

Lee, M.H., Prasad, V. and Lee, D. (2010), "Microfluidic fabrication of stable nanoparticle-shelled bubbles", *Langmuir*, Vol. 26 No. 4, pp. 2227-2230.

Nawar, S., Stolaroff, J.K., Ye, C., Wu, H., Nguyen, D.T., Xin, F. and Weitz, D.A. (2020), "Parallelizable microfluidic dropmakers with multilayer geometry for the generation of

double emulsions", *Lab on a Chip*, Vol. 20 No. 1, pp. 147-154.
Nielsen, A.V., B.M.J.N.G.P. and Woolley, A.T. (2020), "3d printed microfluidics", *Annual Review of Analytical Chemistry*, Vol. 13 No. 1, pp. 45-65.
Nisisako, T., Ando, T. and Hatsuzawa, T. (2012), "High-volume production of single and compound emulsions in a microfluidic parallelization arrangement coupled with coaxial annular world-to-chip interfaces", *Lab on a Chip*, Vol. 12 No. 18, pp. 3426-3435.
Nisisako, T. and Torii, T. (2008), "Microfluidic large-scale integration on a chip for mass production of monodisperse droplets and particles", *Lab Chip*, Vol. 8 No. 2, pp. 287-293.
Rasband, W.S. et al (1997), "Imagej".
Ren, P.W., Ju, X.J., Xie, R. and Chu, L.Y. (2010), "Monodisperse alginate microcapsules with oil core generated from a microfluidic device", *Journal of Colloid and Interface Science*, Vol. 343 No. 1, pp. 392-395.
Romanowsky, M.B., Abate, A.R., Rotem, A., Holtze, C. and Weitz, D.A. (2012), "High throughput production of single core double emulsions in a parallelized microfluidic device", *Lab on a Chip*, Vol. 12 No. 4, pp. 802-807.
Seiffert, S., Thiele, J., Abate, A.R. and Weitz, D.A. (2010), "Smart microgel capsules from macromolecular precursors", *Journal of the American Chemical Society*, Vol. 132 No. 18, pp. 6606-6609.
Suea-Ngam, A., Howes, P.D., Srisa-Art, M. and deMello, A.J. (2019), "Droplet microfluidics: from proof-of-concept to real-world utility?", *Chemical Communications*, Vol. 55 No. 67, pp. 9895-9903.
Tabeling, P. (2005), *Introduction to Microfluidics*, Oxford.
Vijayan, S. and Hashimoto, M. (2019), "3d printed fittings and fluidic modules for customizable droplet generators", *RSC Advances*, Vol. 9 No. 5, pp. 2822-2828.
Vladisavljevic, G.T., Khalid, N., Neves, M.A., Kuroiwa, T., Nakajima, M., Uemura, K., Ichikawa, S. and Kobayashi, I. (2013), "Industrial lab-on-a-chip: design, applications and scale-up for drug discovery and delivery", *Advanced Drug Delivery Reviews*, Vol. 65 Nos 11/12, pp. 1626-1663.
Wagner, J., Tshikhudo, T.R. and Köhler, J.M. (2008), "Microfluidic generation of metal nanoparticles by borohydride reduction", *Chemical Engineering Journal*, Vol. 135, pp. S104-S109.
Weibel, D.B. and Whitesides, G.M. (2006), "Applications of microfluidics in chemical biology", *Current Opinion in Chemical Biology*, Vol. 10 No. 6, pp. 584-591.
Whitesides, G.M. (2006), "The origins and the future of microfluidics", *Nature*, Vol. 442 No. 7101, p. 368.
Zhang, J.M., Aguirre-Pablo, A.A., Li, E.Q., Buttner, U. and Thoroddsen, S.T. (2016), "Droplet generation in cross-flow for cost-effective 3d-printed "plug-and-play" microfluidic devices", *RSC Advances*, Vol. 6 No. 84, pp. 81120-81129.
Zhang, J., Coulston, R.J., Jones, S.T., Geng, J., Scherman, O. A. and Abell, C. (2012), "One-step fabrication of supramolecular microcapsules from microfluidic droplets", *Science*, Vol. 335 No. 6069, pp. 690-694.
Zhang, J., Ji, Q. and Duan, H. (2019), "Three-dimensional printed devices in droplet microfluidics", *Micromachines*, Vol. 10 No. 11, p. 754.

Corresponding author

Peichun Amy Tsai can be contacted at: peichun.amy.tsai@ualberta.ca

For instructions on how to order reprints of this article, please visit our website:
www.emeraldgrouppublishing.com/licensing/reprints.htm
Or contact us for further details: **permissions@emeraldinsight.com**